

MrgX2-Targeting Ligand Screen for Antipseudoallergic Agents by Immobilized His-Tag-Fused Protein Technology

Zhaomin Xia,[#] Qiumei Zhu,[#] Yi Shan, Jiayu Lu, Meidi An, Xiaoxue Mo, Siqi Wang, Wen Yang, Hua Qian, Huaizhen He, and Cheng Wang*Cite This: *J. Med. Chem.* 2025, 68, 5942–5953

Read Online

ACCESS |

Metrics & More

Article Recommendations

Supporting Information



ABSTRACT: Mas-related G protein-coupled receptor X2 (MrgX2) plays a key role in pseudoallergy reactions; thus, it is of great significance to screen compounds with antipseudoallergy activity via MrgX2. Cell membrane chromatography (CMC) demonstrates great potential in drug screening, but it requires further optimization to improve its specificity and stability. In this study, a new CMC system incorporating His-tag-oriented immobilized proteins was constructed to screen MrgX2 antagonists. Single His-tag-fused MrgX2 was extracted intactly and covalently bond to divinyl sulfone-modified amino silica gel to obtain bioaffinity composites. The characterized composites were utilized to establish a MrgX2-His-tag@VS/CMC system to screen MrgX2 antagonists. Compound Z-3578 was screened from a G protein-coupled receptor compound library of 3010 compounds and revealed its efficient antipseudoallergy activity in vitro and in vivo via MrgX2. In conclusion, the new oriented-immobilized CMC system will provide an efficient analytical tool for screening active precursors.

INTRODUCTION

Allergic diseases are a group of allergen-induced immune disorders that initiate various symptoms. Mas-related G protein-coupled receptor X2 (MrgX2), expressed on dorsal root ganglia and human mast cell lines,^{1,2} can be activated by a variety of basic molecules such as substance P (SP), mastoparan, compound 48/80 (C48/80), and neuropeptide Y,³ leading to mast cell degranulation and induces an inflammatory response. It has been reported that activation of MrgX2 modulates inflammatory pain and nonhistamine itching in atopic dermatitis⁴ and is also involved in localized allergic reactions in chronic urticaria.⁵ MrgX2 thus has attracted much attention as a novel drug target,^{1,2,6} which has been the most popular antiallergic target over the past few years. Up to now, MrgX2 diverse antagonists have been found, including natural compounds, saikosaponin A,⁷ imperatorin (IMP)⁸ and rosmarinic acid,⁹ and so forth and synthetic compounds, EP262,¹⁰ diaryl ureas,^{11,12} imperatorin derivatives,¹³ phenalen-naphthalene compounds,^{14,15} and so forth. Beyond that, DNA aptamer¹⁶ and single-stranded oligonucleo-

tide¹⁷ were also demonstrated to possess antiallergic activity via MrgX2. However, there are yet no marketed MrgX2 antagonists, and most of them are still in preclinical research.

Affinity-based drug discovery strategy is an important strategy for drug discovery, which measured the ligand–receptor affinity to reveal its potential bioactivity whether through virtual calculations or actual measurements, such as the molecular docking,¹⁸ biomolecular interaction analysis,¹⁹ and artificial intelligence.²⁰ The biomolecular interaction analysis included classical surface plasmon resonance (SPR),²¹ isothermal titration calorimetry (ITC),²² fluorescence resonance energy transfer (FRET),²³ and emerging cell membrane chromatography (CMC).²⁴ CMC is a bioaffinity

Received: January 25, 2025

Revised: February 24, 2025

Accepted: February 26, 2025

Published: March 4, 2025



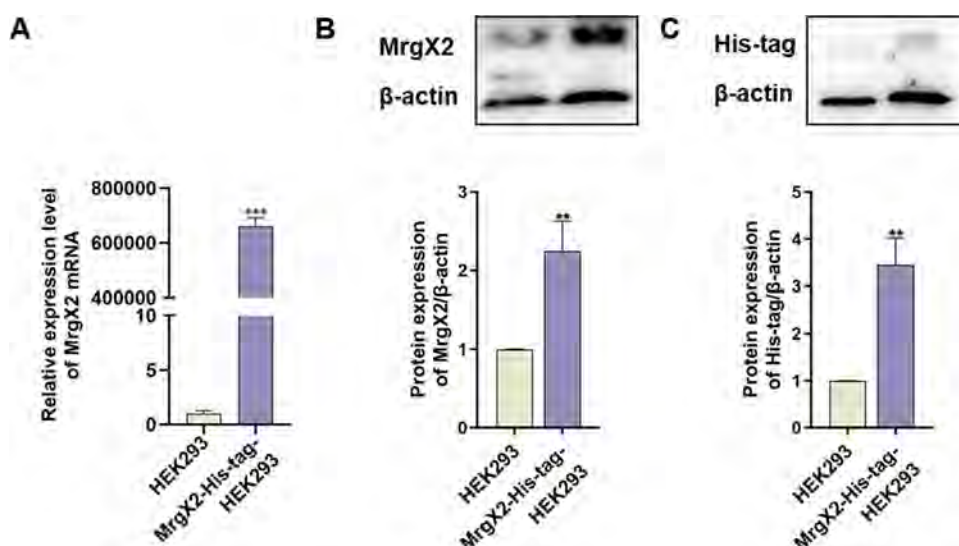


Figure 1. Validation of constructed highly expressing MrgX2-His-tag-HEK293 cells. (A) Quantitative PCR validation of the relative expression level of MrgX2 mRNA; (B) Western blot validation of the protein expression of MrgX2; (C) Western blot validation of the protein expression of His-tag. Data are expressed as mean \pm SEM ($n = 3$). Two-tailed unpaired Student's t test was used to determine significance in statistical comparisons. Differences in data are considered significant, when $**P < 0.01$, $***P < 0.001$, compared to HEK293 cells.

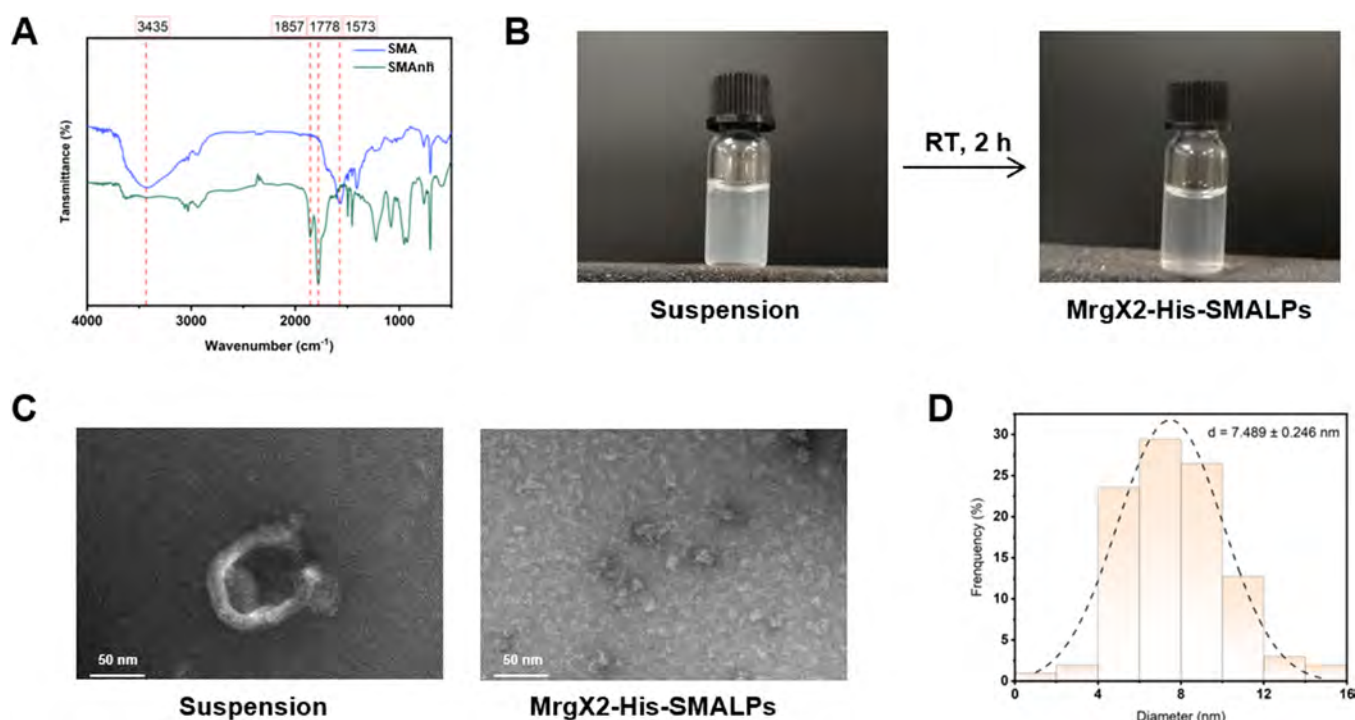


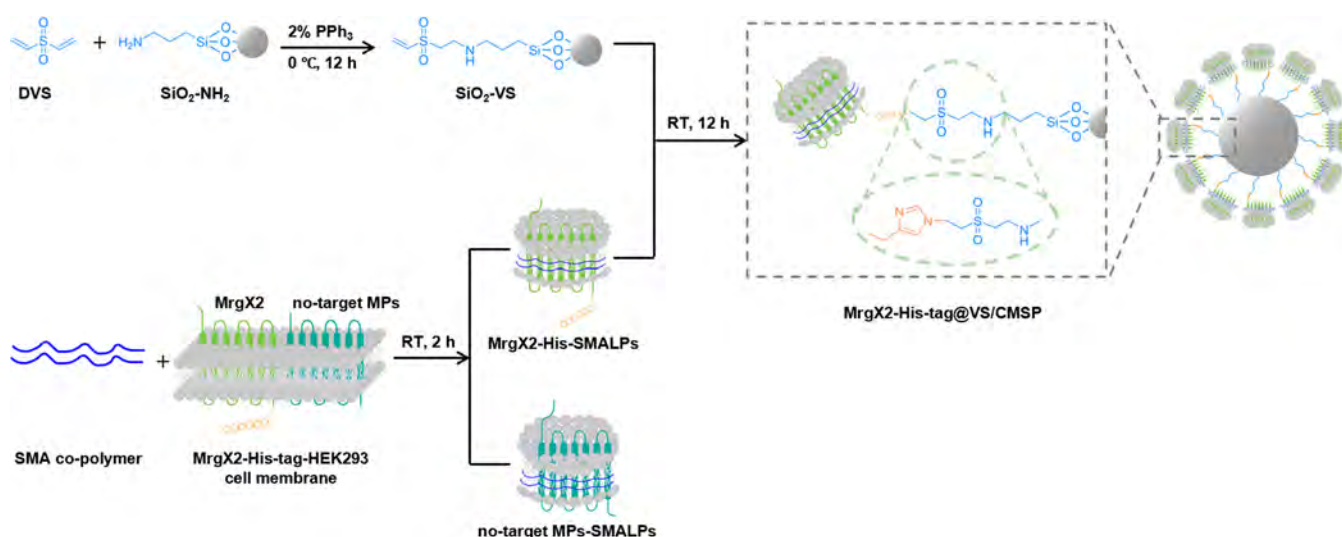
Figure 2. Preparation and characterization of SMA and SMALPs. (A) FT-IR spectra of SMA and SMAnh. (B) Membrane suspension of SMA and MrgX2-His-SMALPs. (C) TEM of the membrane suspension of MrgX2-His-tag and SMA and MrgX2-His-SMALPs. (D) Particle size of MrgX2-His-SMALPs.

chromatographic technique that immobilizes membrane proteins on a chromatographic stationary phase, which mimics the process of drug-ligand interaction in vivo, and provides an efficient and convenient tool for drug discovery.^{24–26} Protein immobilization played an essential role in CMC, and affinity tag coupling has been proved to achieve site-specific covalent immobilizing proteins under milder conditions.²⁷ Histidine affinity tag (His-tag) is currently the most popular tag used for protein purification due to its small size (0.84 kDa) and minimal interference with protein expression and folding

functions,²⁸ accurate for revealing receptor-drug interactions.²⁹ Additionally, an amphiphilic polymer styrene maleic acid (SMA) copolymer was recently used to extract of functional membrane proteins while preserving their natural lipid environment, forming natural nanodiscs known as styrene-maleic acid lipid particles (SMALPs),^{30–33} which has been widely used to solubilize G protein-coupled receptors (GPCRs) in vitro.³⁴

In this study, a new CMC system incorporating immobilized His-tag fused protein technology was constructed to screen

Scheme 1. Schematic Diagram of the Construction of MrgX2-His-tag@VS/CMSP



MrgX2 antagonists. Single His-tag fused MrgX2 was extracted intactly by SMA and covalently bonded to divinyl sulfone (DVS)-modified amino silica gel to obtain bioaffinity composites, which were utilized to establish an MrgX2-His-tag@VS/CMC system to screen MrgX2 antagonists, from a GPCR compound library of 3010 compounds. The screened potential candidates were evaluated for their antipseudoallergic activities via *in vitro* cell degranulation assays and an *in vivo* mice allergy model.

RESULTS AND DISCUSSION

Validation of Constructed Highly Expressing MrgX2-His-tag-HEK293 Cells. MrgX2-His-tag-HEK293 cells, characterized by high expression levels of MrgX2, were constructed by fusing a His-tag onto the C-terminal end of MrgX2. Quantitative PCR and Western blotting assays were used to detect the changes in the mRNA and protein expression levels of MrgX2. As shown in Figure 1A, the relative mRNA expression level of MrgX2-His-tag-HEK293 cells was found to be 660561.5-fold higher than that of wild-type HEK293 cells. Additionally, the protein expression of MrgX2 in the MrgX2-His-tag-HEK293 cells was significantly elevated, exhibiting a 2.2-fold increase compared to that in wild-type HEK293 cells (Figure 1B), and the His-tag increased by 3.5-fold (Figure 1C). The above results indicated that the MrgX2-His-tag-HEK293 cell line was successfully constructed.

Preparation of MrgX2-His-SMALPs. SMA was prepared by hydrolysis of SMA copolymers³³ and used to extract MrgX2, resulting in forming natural nanodiscs to maximize preservation of the natural structure of MrgX2.³⁰ SMA was generated by mixing styrene maleic anhydride (SMAnh) with a NaOH solution, and the disappeared stretching vibration absorption at 1857 and 1778 cm^{-1} and observed absorption peaks at 1573 and 3435 cm^{-1} indicated the successful transition from SMAnh to SMA (Figure 2A). MrgX2 and other proteins were then independently extracted from the cell membrane in an SMA solution, forming MrgX2-His-tag SMA lipid particles (MrgX2-His-SMALPs) and nontarget protein SMA lipid particles (nontarget MPs-SMALPs), becoming a clearer membrane suspension (Figure 2B). In this way, MrgX2 and other nontarget proteins were separated, and the SMALP has a more consistent size at 7.489 ± 0.246 nm (Figure 2C,D),

which was basically in accordance with the reported average diameter of SMALPs at 8–9 nm.³⁵

Synthesis and Characterizations of MrgX2-His-tag@VS/CMSP. His-tag was reported to be a covalent bond with divinyl sulfone (DVS).^{36,37} SiO_2 -VS was synthesized by binding DVS on the surface of SiO_2 - NH_2 and further mixed with a solution of MrgX2-His-SMALPs for oriented immobilization of MrgX2-His-SMALPs on the SiO_2 -VS surface, forming the MrgX2-His-tag@VS/CMSP, as depicted in Scheme 1. This kind of covalent immobilization offers the following advantages: SMA extracted minimal MrgX2 units and maintained its activity; only His-tagged MrgX2 can bind to the surfaces, effectively preventing nontarget proteins binding; the intracellular His-tag bond to SiO_2 -VS facilitated the directional immobilization of MrgX2, outward exposing its extracellular active pockets.

The prepared MrgX2-His-tag@VS/CMSP was characterized by SEM, TEM, and XPS. Compared with the smooth and uncovered surfaces of SiO_2 - NH_2 and SiO_2 -VS, MrgX2-His-tag-SMALPs exhibited obvious traces of membrane adhesion (Figure 3A) and distinct translucent membrane cover (Figure 3B). XPS showed a significant increase of C 1s, N 1s, and P 2p in the SiO_2 -VS and MrgX2-His-tag@VS, compared to SiO_2 - NH_2 (Figure 3C-a–d); the observed characteristic peak of S 2p (Figure 3C-e) and C 1s peaks of C–C, C–O, and C=O at 288.0, 285.7, and 284.5 eV (Figure 3C-f) in MrgX2-His-tag@VS comprehensively indicated the successful binding of MrgX2-His-tag@SMALPs onto the VS- SiO_2 surface.

System Suitability of MrgX2-His-tag@VS/CMC System. An MrgX2-His-tag@VS/CMC system was established by using the prepared MrgX2-His-tag@VS/CMSP. (R)-ZINC-3573, a highly selective MRGPRX2 agonist, exhibited strong retention on the MrgX2-His-tag@VS/CMC system, while negative drug, including metoprolol (β_1 -receptor antagonist), erlotinib (EGFR antagonist), and captopril (ACE inhibitor), did not (Figure 4A), confirming the selectivity of the MRGPRX2-His-tag@VS/CMC system for MRGPRX2 ligands. Meanwhile, three MrgX2 agonists, (R)-ZINC-3573, sinomenine, and ciprofloxacin, showed significantly retention on the MrgX2-His-tag@VS/CMC system but not on the SiO_2 -VS/CMC system (Figure 4B). This revealed the specificity of the MRGPRX2-His-tag@VS/CMC system that the retention

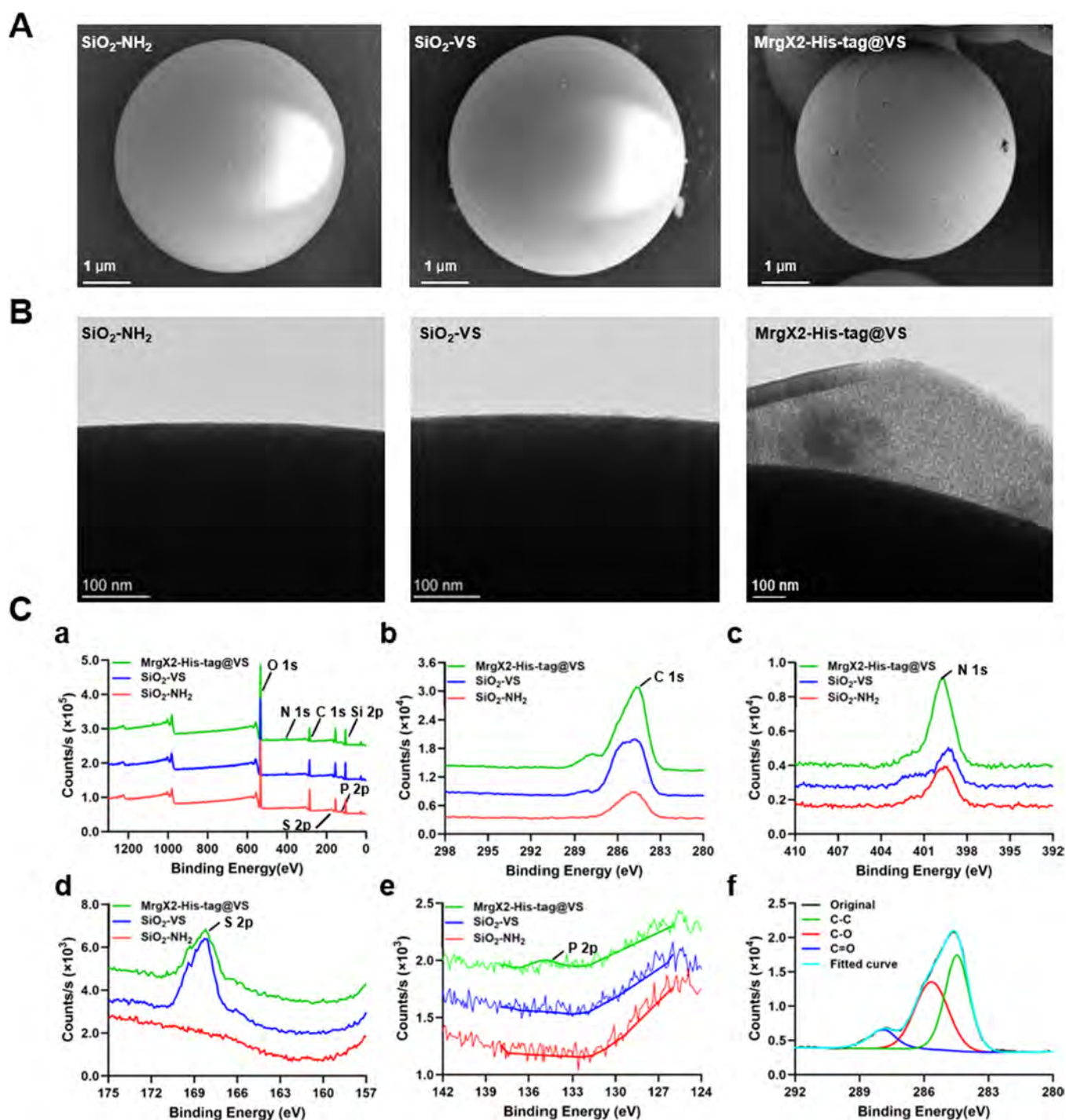


Figure 3. Characterization of MrgX2-His-tag@VS/CMSP. (A) Surface characterization of the silica gels by SEM, SiO₂-NH₂, SiO₂-VS, and MrgX2-His-tag@VS/CMSP. Scale bar: 1 μm. (B) Fine structure characterization of the silica gels by TEM, SiO₂-NH₂, SiO₂-VS, and MrgX2-His-tag@VS/CMSP. Scale bar: 100 nm. (C) Surface analysis of SiO₂-NH₂, SiO₂-VS, and MrgX2-His-tag@VS/CMSP by XPS: (a) XPS survey-scan; (b) C 1s; (c) N 1s; (d) S 2p; (e) P 2p ($n = 3$); (f) fitted curve of C 1s of MrgX2-His-tag@VS/CMSP.

properties were entirely attributed to their interaction with immobilized MrgX2. Additionally, the MrgX2-His-tag@VS/CMC system exhibited desirable intercolumn reproducibility (RSD = 5.78%, $n = 3$) (Figure 4C), intracolumn reproducibility 5.06% ($n = 5$) (Figure 4D), and robust column activity (Figure 4E), according to the retention time of (R)-ZINC-3573.

Application of the MrgX2-His-tag@VS/CMC System to Screen Antipseudoallergic Drugs. The established

MrgX2-His-tag@VS/CMC system was utilized to identify MrgX2 antagonists from the Express-Pick Library (L3600), which is a GPCR compound library. A total of 3010 compounds were systematically combined in groups of 10, yielding 301 distinct mixtures, which were subsequently introduced into the MrgX2-His-tag@VS/CMC system. A total of 48 mixtures, comprising 480 compounds, demonstrated favorable retention characteristics and were utilized to examine for the β -aminohexosidase release ability on LAD2

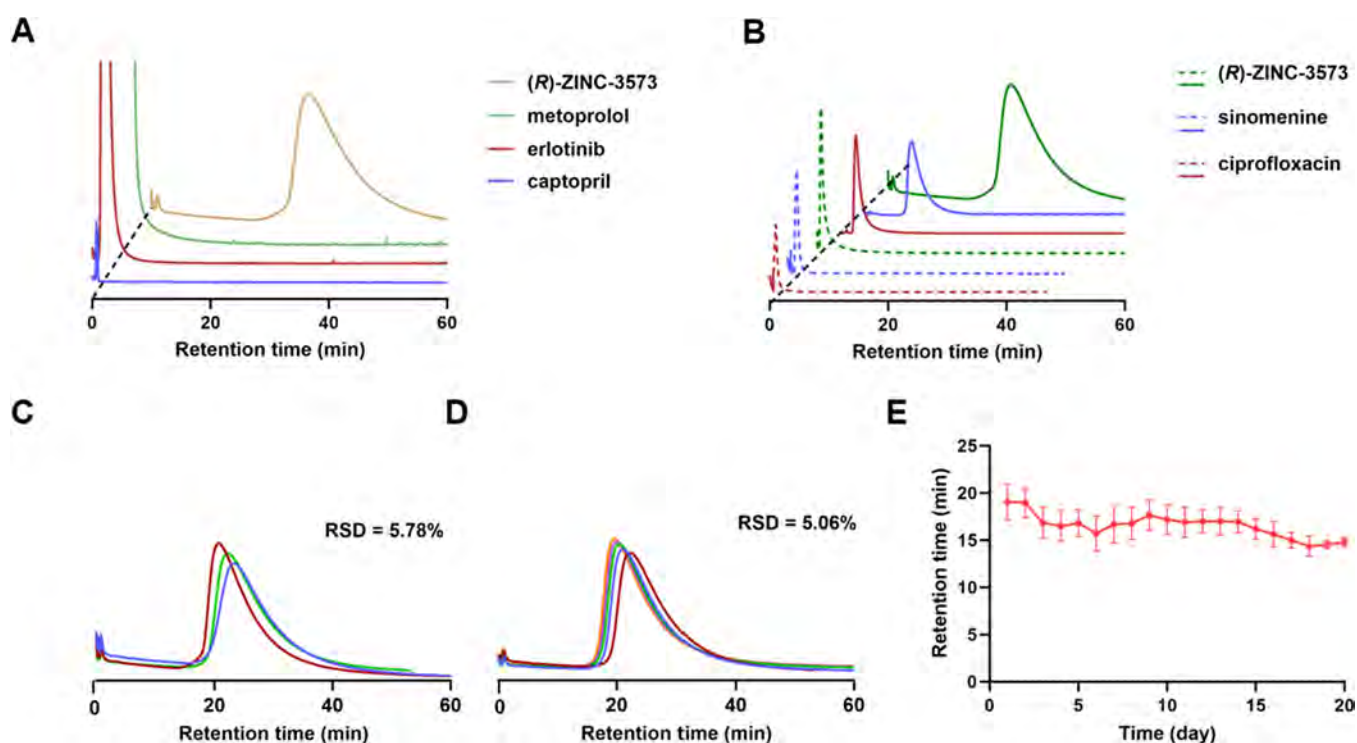


Figure 4. System applicability of the MrgX2-His-tag@VS/CMC system. (A) Selectivity of the MrgX2-His-tag@VS/CMC system. Retention behavior of metoprolol, erlotinib, captopril, and (R)-ZINC-3573 on the MrgX2-His-tag@VS/CMC system. (B) Specificity of the MrgX2-His-tag@VS/CMC system. Retention behavior of sinomenine, ciprofloxacin, and (R)-ZINC-3573 was measured on the MrgX2-His-tag@VS/CMC system (solid line) and on the VS-SiO₂-VS/CMC system (dashed line). (C) Inter-column reproducibility, $n = 3$. (D) Intra-column reproducibility, $n = 5$. (E) Column lifetime of MrgX2-His-tag@VS/CMC system, $n = 3$.

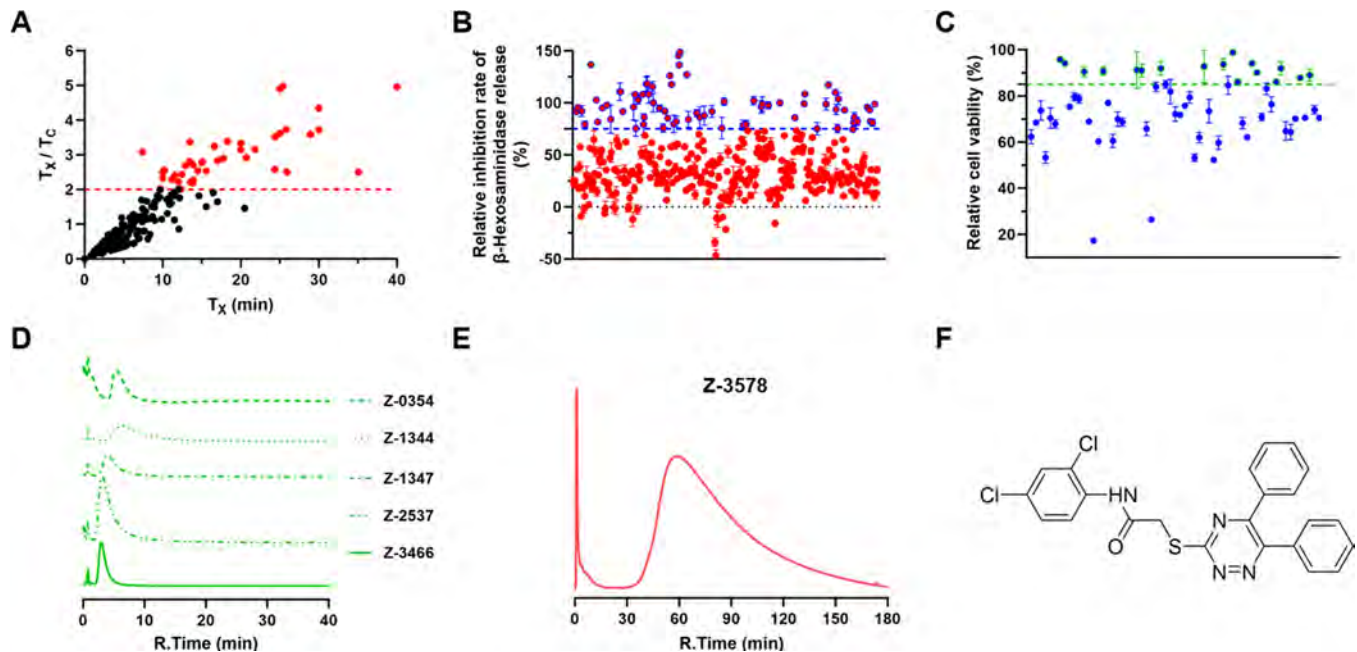


Figure 5. MrgX2-His-tag@VS/CMC system for screening compound library. (A) Relative retention of mixed compounds ($n = 301$) in group of 10 in the MrgX2-His-tag@VS/CMC model. T_x : retention time of mixed compounds on the MrgX2-His-tag@VS/CMC system; T_c : retention time of (R)-ZINC-3573 on the MrgX2-His-tag@VS/CMC system. (B) Compounds with twice the retention time of (R)-ZINC-3573 on the MrgX2-His-tag@VS/CMC system inhibited SP-induced β -aminohexosidase release from LAD2 cells at a concentration of 50 μ M ($n = 400$). (C) Cell viability of compounds that effectively inhibited β -aminohexosidase release by up to 75% at 50 μ M ($n = 71$). (D) Retention behavior of Z-0354, Z-1344, Z-1347, Z-2537, and Z-3466 on the MrgX2-His-tag@VS/CMC system. (E) Retention behavior of Z-3578 on the MrgX2-His-tag@VS/CMC system. (F) The structure of Z-3578. Values are expressed as mean \pm SEM ($n = 3$).

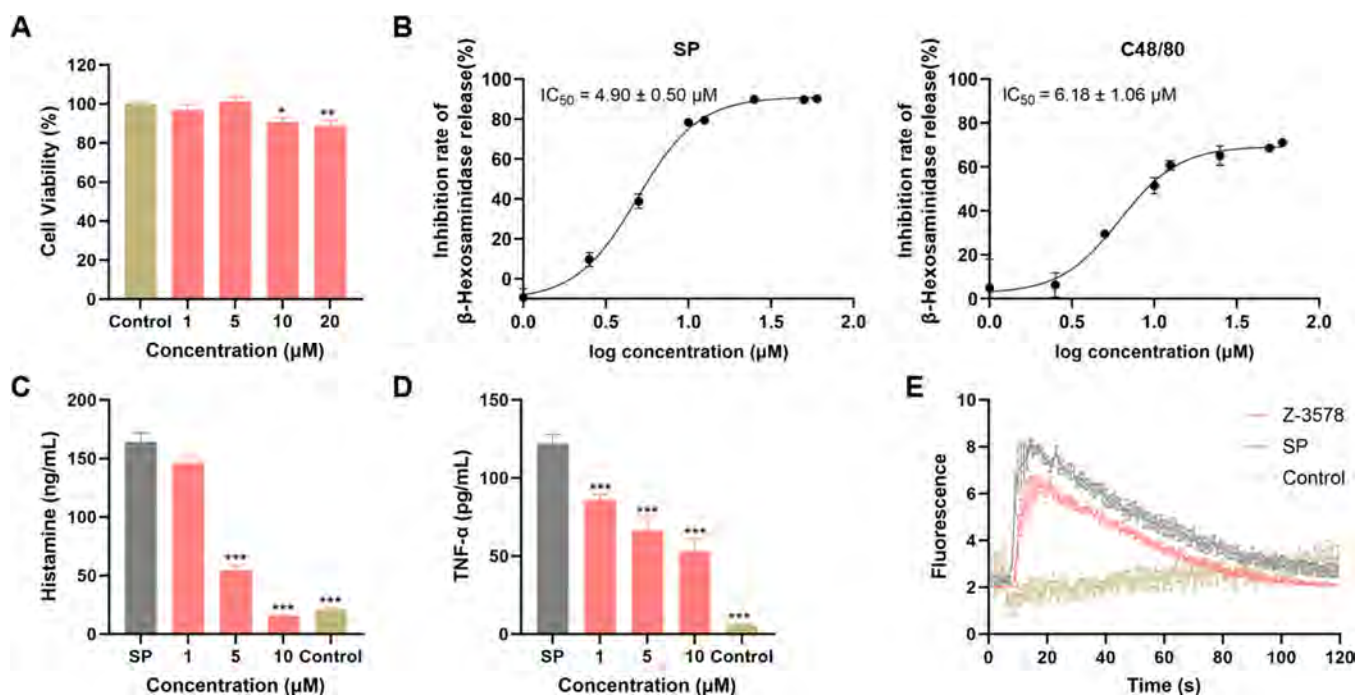


Figure 6. Evaluation of the cell viability and antipseudoallergic effect of compound Z-3578. (A) The cell viability of compound Z-3578 in LAD2 cells. (B) The IC_{50} of compound Z-3578 inhibited the β -hexosaminidase release induced by SP and C48/80 in the LAD2 cell. (C) The histamine release inhibited by compound Z-3578 at 1, 5, and 10 μ M compared with the SP group. (D) The TNF- α release inhibited by compound Z-3578 at 1, 5, and 10 μ M compared with the SP group. (E) Compound Z-3578 inhibited calcium mobilization of MrgX2-His-tag cells at 10 μ M. Values are expressed as mean \pm SEM. Multiple group comparisons were performed using ANOVA with a Dunnett's post hoc test. Differences in data are considered significant when * P < 0.05, ** P < 0.01, *** P < 0.001, compared to control (cell viability) or SP (n = 3).

cells in an individual compound (Figure 5A). Seventy compounds effectively inhibited the SP-induced β -aminohexosidase release (75%) at a concentration of 50 μ M (Figure 5B). Among them, 19 compounds showed low cytotoxicity with cell viability greater than 85% (Figure 5C), six out of them exhibiting significant retention properties on the MrgX2-His-tag@VS/CMC system, namely, compounds Z-0354, Z-1344, Z-1347, Z-2537, Z-3466, and Z-3578 (Figure 5D,E). The most potential compound Z-3578 (Figure 5F) was selected to investigate for its antiallergic activity in vitro and in vivo.

Compound Z-3578 Inhibited Degranulation and Inflammatory Factor Release in Mast Cells. When pseudoallergic reactions occur, mast cells (MCs) are activated to degranulate, releasing a range of inflammatory mediators such as β -hexosaminidase, histamine, and cytokines.^{38,39} SP and C48/80, two MrgX2 agonists, can induce degranulation of MCs.⁴⁰ Without obvious cell cytotoxicity (Figure 6A), compound Z-3578 effectively inhibited SP and C48/80-induced β -aminohexosidase release in a concentration-dependent manner, with half inhibitory concentration (IC_{50}) values of 4.90 ± 0.50 and 6.18 ± 1.06 μ M (Figure 6B), respectively. Moreover, Z-3578 exhibited remarkably reduced histamine and cytokine TNF- α release in a concentration-dependent manner (Figure 6C,D). The activation of MrgX2 is concomitant with calcium mobilization, and 10 μ mol/L Z-3578 also resulted in diminished calcium mobilization (Figure 6E). The above in vitro results indicated that compound Z-3578 possessed potential antagonistic activity against pseudoallergic reactions.

Compound Z-3578 Inhibited Pseudoallergic Response in Mice. MrgB2, the mouse homologue of MrgX2, was used to further evaluate the antipseudoallergic activity of

compound Z-3578 via in vivo model of local allergic reactions. Z-3578 substantially decreased the thickness of mice paws at 0.5 and 1.0 mg/mL (Figure 7A,B) and reduced the Evans blue extravasation at 1.0 mg/mL (Figure 7A,C), compared to the C48/80 group. Toluidine blue staining revealed that Z-3578 could attenuate the mast cell degranulation induced by C48/80 in mice (Figure 7E), which was in accordance with the paw swelling and Evans blue extravasation. Additionally, Z-3578 substantially decreased serum histamine release in mice (Figure 7D). These results indicate that Z-3578 was capable of inhibiting pseudoallergic reactions in both mast cells and mice.

Binding Properties between the Potential Compound Z-3578 and MrgX2. Protein-based affinity chromatography has been widely used for detecting ligand–receptor interactions.^{6,41–43} To further investigate the interaction between Z-3578 and MrgX2, frontal analysis was first used to examine the binding affinity of Z-3578 with MrgX2. The breakthrough curve was gradually moved forward as the increasing concentration of compound Z-3578, indicating the saturation of the ligand–receptor interaction, and the K_D value was calculated as $1.41 \pm 0.73 \times 10^{-5}$ mol/L (Figure 8A). Furthermore, zonal elution was used to investigate the competitive binding of compound Z-3578 with (R)-ZINC-3573. With the increasing concentration of (R)-ZINC-3573 ranging from 0 to 1.0×10^{-7} mol/L, the retention times of compound Z-3578 were decreased from 58.73 to 23.73 min (Figure 8B), respectively, which indicated that compound Z-3578 exhibited competitive binding effect with (R)-ZINC-3573 to MrgX2. The classical SPR assay was also used to determine the binding ability between Z-3578 and MrgX2, and the K_D value was calculated as 7.29×10^{-7} mol/L (Figure 8C).

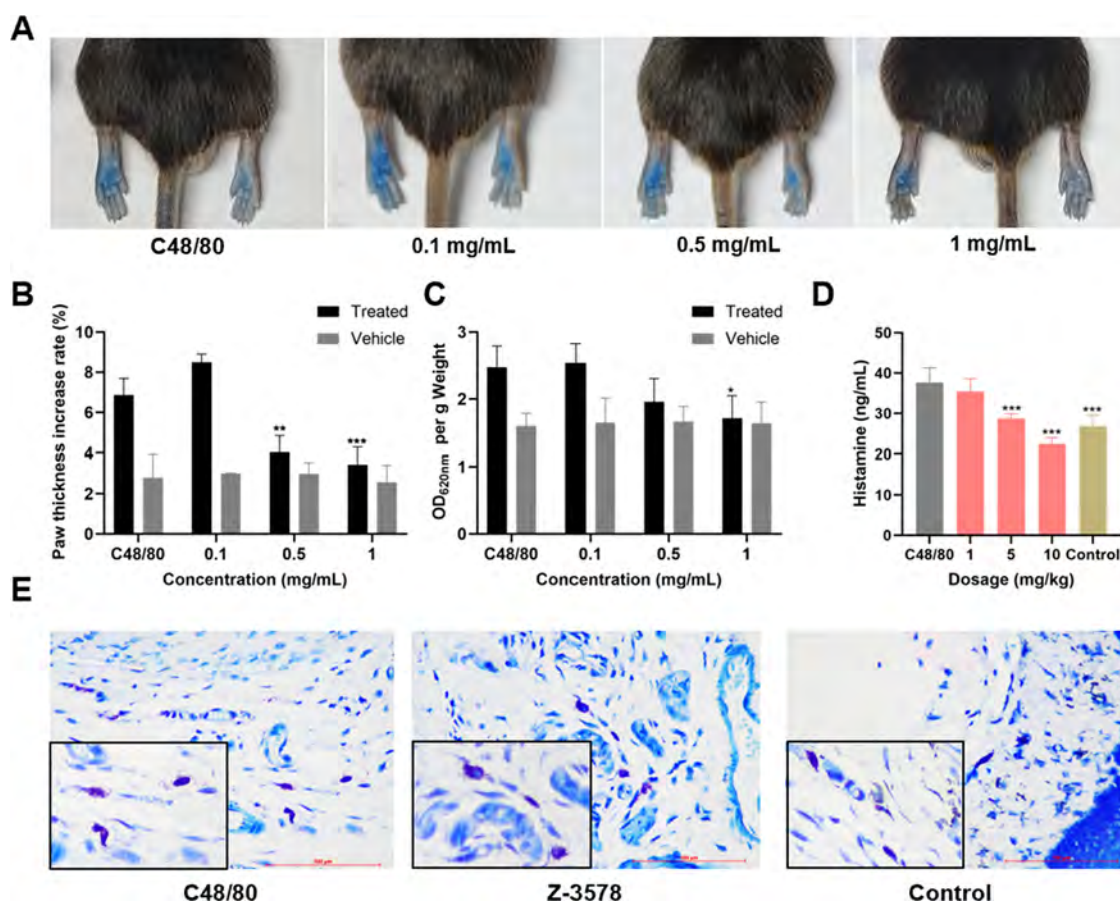


Figure 7. Compound Z-3578 inhibited C48/80-induced pseudoallergic reactions in vivo. (A) Representative pictures of paw swelling and Evans blue exudation in mice; left paw: injection of C48/80; right paw: injection of saline. (B) Rates of paw swelling in mice. (C) Rates of Evans blue exudation in mice. (D) Effect of compound Z-3578 on C48/80-induced histamine release in mice. (E) Toluidine blue staining of the skin of the paws of the mice. Values are expressed as mean \pm SEM. Multiple group comparisons were performed using ANOVA with a Dunnett's post hoc test. Differences in the data are significant when * $P < 0.05$, ** $P < 0.01$, *** $P < 0.001$, when compared with the C48/80 group ($n = 5$).

The interaction pattern of Z-3578 with MrgX2 was further explored by molecular docking. Z-3578 and (R)-ZINC-3573 bound in the same cavity of the MrgX2 (Figure 8D) and formed a strong hydrogen bond with amino acid residue Trp243 at a length of 1.9 Å (Figure 8E). This result was consistent with the previous reference of MrgX2 agonists.⁴⁴ All in all, compound Z-3578 demonstrated a robust binding affinity to MrgX2.

CONCLUSIONS

In this study, we developed a small-molecule ligand screening system, designated as the MrgX2-His-tag@VS/CMC system, which leverages the innovative fusion of His-tag and SMA technology. This system demonstrated robust column performance, desirable specificity, promising selectivity, and significantly prolonged stability. It was effectively employed to screen for MrgX2 antagonists within a GPCR compound library comprising 3010 compounds. Compound Z-3578 emerged as a potential MrgX2 antagonist, exhibiting significant inhibitory effects on the release of β -aminohexosidase, histamine, and inflammatory mediators in LAD2 cells, as well as effectively alleviating allergic reactions in mice. In conclusion, this novel oriented-immobilized CMC system represents a promising platform for the screening of potential small-molecule compounds and offers an innovative strategy for the identification and discovery of active precursors.

METHODS

Compounds and Reagents. Fetal bovine serum (FBS) was obtained from Hyclone (Utah, USA). Penicillin–streptomycin solution was purchased from Xi'an Hat Biotechnology Co., Ltd. (Xi'an, China). Puromycin was procured from Meilunbio (Dalian, China). MrgX2 antibody (ab237047) and His-tag (666005–1-1g) were purchased from Abcam (Cambridge, UK) and Proteintech (Wuhan, China), respectively. Express-Pick Library (L3600) was purchased from Selleck Chemicals LLC (Houston, USA). Substance P was synthesized by NJ Peptide Co., Ltd. (Nanjing, China). (R)-ZINC-3573 was obtained from TOCRIS (Bristol, UK). Compound 48/80 (C48/80), *p*-nitrophenyl-*N*-acetyl- β -D-glucosamide, Triton X-100, and histamine were purchased from Sigma-Aldrich (St. Louis, MO). The purity of the synthesized product was >98%. *d*₄-HA-12HCl (A, A, B, B-D₄, 98%) was purchased from Cambridge Isotope Laboratories, Inc. (MA, USA). The Fluo-3 AM/calcium ion fluorescent probe was procured from GeneCopoeia (Maryland, USA). The TNF- α Array kit was purchased from Sino Biological Inc. (Beijing, China). All purified water was purchased from the Hangzhou Wahaha Group Co., Ltd.

Hypotonic buffer A (2 mM EDTA and 2 μ L/mL proteinase inhibitor, 20 mM PBS, pH = 7.4), hypotonic buffer B (150 mM NaCl, 10% (v/v) glycerol, 20 mM Tris-HCl, pH = 8), tyrode's solution (TM buffer: NaCl 119 mM, KCl 4.7 mM, CaCl₂ 2.5 mM, MgSO₄ 1.1 mM, KH₂PO₄ 1.1 mM, HEPES 10 mM, glucose 5 mM, BSA 6.3 mM, pH 7), and calcium imaging buffer (CIB: NaCl 125 mM, KCl 3 mM, CaCl₂ 2.5 mM, MgCl₂ 0.6 mM, HEPES 10 mM, glucose 20 mM, NaHCO₃ 1.2 mM, sucrose 20 mM, pH 7.4) were prepared separately

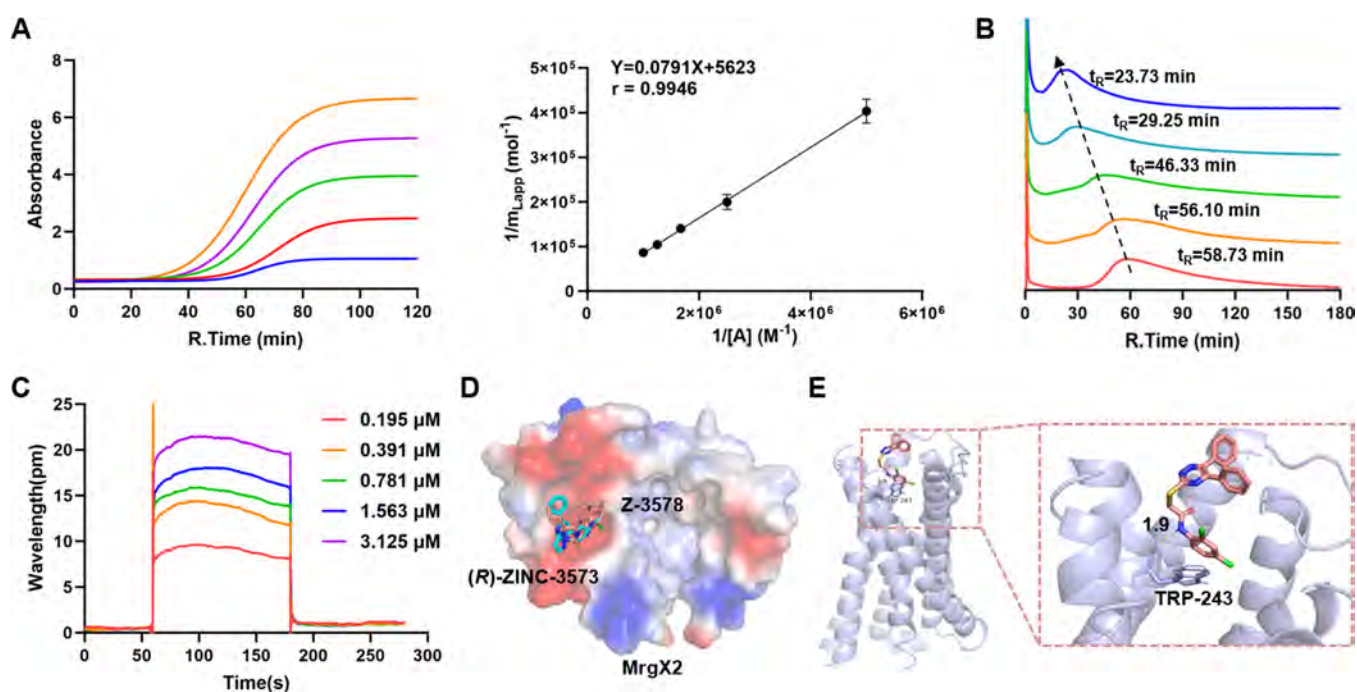


Figure 8. Examination of the binding properties of Z-3578 with MrgX2. (A) MrgX2-His-tag@VS/CMC breakthrough curve of compound Z-3578 and the regression curves achieved by plotting $1/m_{Lapp}$ vs $1/[A]$. The concentrations of Z-3578 were 2×10^{-7} , 4×10^{-7} , 6×10^{-7} , 8×10^{-7} , and 1×10^{-6} mol/L (from bottom to top). Each point with a horizontal bar represents the mean \pm SEM ($n = 3$). (B) Elution profiles of compound Z-3578 on the MrgX2-His-tag@VS/CMC column with different concentrations of (R)-ZINC-3573. The concentrations of compound Z-3578 were 0, 2.0×10^{-8} , 4.0×10^{-8} , 8.0×10^{-8} , and 1.0×10^{-7} mol/L (from bottom to top). (C) Measurement of binding affinities between the compounds Z-3578 and MrgX2 by the surface plasmon resonance assay. (D) Electrostatic surface representation of the MrgX2 extracellular pocket with Z-3578 and (R)-ZINC-3573. Compound Z-3578 is pink, and (R)-ZINC-3573 is cyan. (E) Molecular docking of compound Z-3578 with MrgX2. Compound Z-3578 is pink, MrgX2 is purple, and the yellow color is the hydrogen bond.

before the experiments. Stop buffer was made up of 0.1 M Na_2CO_3 and 0.1 M NaHCO_3 (9:1).

Cell Lines and Cell Culture Conditions. The MrgX2-His-tag cell line was constructed at Genomeditech (Shanghai, China). The expressing cell line details are shown in the [Supporting Information](#). MrgX2-His-tag cells were maintained in DMEM with 10% FBS, 100 U/mL penicillin, 100 $\mu\text{g}/\text{mL}$ streptomycin, and 0.75 $\mu\text{g}/\text{mL}$ puromycin.

The LAD2 cells kindly provided by Dr. A. Kirshenbaum and Dr. D. Metcalfe (NIH, USA) were cultured in StemPro-34 medium supplemented with 10 mL/L of StemPro nutrient supplement, 1:100 penicillin–streptomycin, 2 mM L-glutamine, and 100 ng/mL of human stem cell factor at 37 °C with 5% CO_2 .

Mouse Models. Adult male C57BL/6 (6–8 weeks) mice were purchased from the Medical Laboratory Animal Center of Xi'an Jiaotong University. The mice had unrestricted access to food and water and were kept in an environment with temperatures of 20–25 °C, 50–60% air humidity, and light and darkness cycling every 12 h. The experimental protocols for mice were approved by the Animal Ethics Committee at Xi'an Jiaotong University, Xi'an, China (permit number: XJTU 2019–714).

Preparation and Characterization of MrgX2-His-tag-SMALPs. A 5 g portion of SMA2000 powder was dissolved in 50 mL of 1 M NaOH solution at room temperature and then stirred overnight. The solution was refluxed for 2 h and then cooled. Then concentrated hydrochloric acid was then slowly added to the solution to precipitate the polymer, which was washed four times with purified water (3×20 mL). After an additional 60 mL of 0.6 M NaOH solution was added to dissolve the polymer, the pH of the mixture was adjusted to 8, and the mixture was dried in an oven at 40 °C. The SMA powder was characterized by Fourier transform infrared spectroscopy (FT-IR) (Nicolet Nexus-410, Madison, USA).

MrgX2-His-tag cells (1×10^7) were digested with trypsin and then washed twice with phosphate-buffered saline (PBS). The cells were

resuspended with 3 mL of buffer A, sonicated for 30 min, and centrifuged at 1500 rpm for 5 min at 4 °C, and the supernatant was collected. After adding 2 mL of hypotonic buffer to resuspend the precipitate, the mixture was homogenized at 4 °C for 20 min and then centrifuged at 1500 rpm for 5 min to collect the supernatant. The two supernatants were combined and centrifuged at 12,000 rpm for 20 min. Also, the wet weight of the membrane was calculated.

Membranes were resuspended at a concentration of 30 mg/mL in buffer B. SMA powder was added to the resuspension membrane solution to give a final concentration of 2.5% (w/v), and the solution was incubated for 2 h at 25 °C. After the membrane solution was centrifuged at 12,000 rpm for 20 min at 4 °C, the supernatant containing SMALPs was collected. SMALP suspensions were characterized by using negative staining transmission electron microscopy (TEM, JEM-1400, JEOL, Japan).

Preparation and Characterization of MrgX2-His-tag@VS/CMSP. At 0 °C, 0.5 g of $\text{SiO}_2\text{-NH}_2$ and 114 μL of DVS were added to 20 mL of *N,N*-dimethylformamide with 5.98 mg of 2% triphenylphosphine (PPh_3) as a catalyst. Then, the mixture was stirred at 0 °C for 12 h. The product was washed three times alternately with purified water and acetonitrile and then dried at 85 °C to obtain the $\text{SiO}_2\text{-VS}$.

A 50 mg portion of $\text{SiO}_2\text{-VS}$ was added to the SMALP solution and stirred at 25 °C for 12 h. The mixture was centrifuged at 5000g for 5 min to get the CMSP, which was resuspended with 2 mL of purified water to obtain MrgX2-His-tag@VS/CMSP. The stationary phases were verified by scanning electron microscopy (SEM, GEMINI 500, ZEISS), transmission electron microscopy (TEM, JEM-1400, JEOL, Japan), and X-ray photoelectron spectroscopy (XPS, ESCALAB 206 250xi spectrometer, Thermo Fisher, USA).

Systemic Applicability of the MrgX2-His-tag@VS/CMC System. The prepared MrgX2-His-tag@VS/CMSP was loaded into a chromatography column (10×2.0 mm i.d.) by the method of wet packing to create the MrgX2-His-tag@VS/CMC column. Subsequently, compounds acting on other receptors, captopril, erlotinib,

and metoprolol, were used as negative controls, and (*R*)-ZINC-3573 was used as a positive control to validate the selectivity of the MrgX2-His-tag@VS/CMC column. The specificity of the (*R*)-ZINC-3573,⁴⁵ ciprofloxacin,⁴⁶ and sinomenine⁴⁷ on the MrgX2-His-tag@VS/CMC column and the SiO₂-VS/CMC column was assessed by comparing the retention time. Intercolumn repeatability was assessed by injecting (*R*)-ZINC-3573 solution into three different MrgX2-His-tag@VS/CMC columns, and intracolumn repeatability was assessed by injecting (*R*)-ZINC-3573 solution into the same column five times in a row. The relative standard deviation (RSD) of retention time was calculated to evaluate the intracolumn and intercolumn repeatability. Finally, daily injections of (*R*)-ZINC-3573 were performed to investigate the lifespan of the column, which was assessed against the change in retention behavior of the (*R*)-ZINC-3573.

Application of the System for Screening of Small-Molecule Compound Library. Each group of 10 compounds from the compound library was combined to create a 20 μ L blended sample, with 0.5 μ L of each compound aspirated and diluted with 15 μ L of methanol. Mixed samples exhibiting significant retention properties on the MrgX2-His-tag@VS column were examined for the β -aminohexosidase release of individual compounds. Additionally, the cell viability of the compounds was assessed in conjunction with screening antipseudoallergic compounds. LC-2030C (Shimadzu, Japan) was used for CMC drug screening. The screening process of small-molecule compound was carried out using the following chromatographic conditions: MrgX2-His-tag@VS/CMC column (10 \times 2.0 mm i.d.); mobile phase: 5 mM Na₂HPO₄ solution; column temperature: 37 $^{\circ}$ C; detector: diode array detector; injection volume: 3 μ L; flow rate: 0.2 mL/min.

Cell Viability Assay. LAD2 cells (2×10^4 cells per well) were seeded in a 96-well plate and treated with different concentrations of the compounds. Five replicate wells were set up for each concentration. The plate was incubated at 37 $^{\circ}$ C with 5% CO₂ for 24 h, and then, each well was treated with 10 μ L of CCK8 (mishushengwu, Xi'an, China) for 2 h. The optical density (OD) of each well was measured at 450 nm, and the LAD2 cell viability was calculated using the following formula:

$$\text{cell viability} = \frac{\text{OD}_{\text{treated}} - \text{OD}_{\text{blank}}}{\text{OD}_{\text{control}} - \text{OD}_{\text{blank}}} \times 100\%$$

β -Hexosaminidase Release Assay. LAD2 cells (5×10^4 cells per well) were seeded into 96-well plates and cultivated for 2 h in the incubator. After centrifuging at 2000 rpm for 5 min, the supernatant was discarded. Different concentrations of the compounds prepared with TM buffer were added to the wells, and the TM buffer was added in blank control and positive control wells. The plate was incubated for 30 min. Then, the positive compound was added to the wells to stimulate the cell. Also, the blank group was added to the same volume TM buffer. Then, the plate was incubated for another 30 min and centrifuged at 2000 rpm for 5 min. Fifty microliters of supernatant was pipetted into a new plate, and the rest of the supernatant in blank was discarded. The blank wells were lysed with 100 μ L of 0.1% Triton X-100 and centrifuged at 2000 rpm for 5 min, and 50 μ L of supernatant was also aspirated. Then, 50 μ L of *p*-nitrophenyl *n*-acetyl- β -D-glucosamide in 0.1 M citric acid/sodium citrate buffer (pH = 4.5) was added to the supernatants and the plate was incubated for 2 h. The stop buffer (0.1 mM Na₂CO₃/NaHCO₃) was added, and the plate was measured at 405 nm by a microplate reader. The percentage of β -hexosaminidase released was calculated as the absorbance of the culture supernatant/absorbance of the total cell lysate supernatant \times 100%.

Histamine Release Assay. The treatment of histamine release was similar to that of the β -hexosaminidase assay. SP was used as an agonist. After incubation with compound Z-3578, the supernatant was collected and then 50 ng/mL *d*₄-HA in acetonitrile was added. The mixture was centrifuged at 12,000 rpm for 20 min at 4 $^{\circ}$ C. The supernatant was collected, filtered, and analyzed for histamine content using UHPLC-ESI-MS/MS.

Intracellular Ca²⁺ Mobilization Assay. MrgX2-His-tag cells (1×10^4 cells per well) were seeded in the 96-well plates and incubated for 12 h. Then, the medium was discarded, and the plate was washed twice with CIB buffer. The compound Z-3578 was prepared to a concentration of 10 μ M with the incubation buffer (3.5 mM Fluo-3 AM, 0.1% [w/v] F-127, diluted with CIB), and the incubation buffer was added in the blank group. After being incubated for 30 min, the supernatant of the plate was discarded, and the cells were washed twice with CIB. The fluorescent microscope (Nikon, Ti-U, Japan) was used to record cell dynamic changes of fluorescence intensity.

Chemokine Release Assay. The mixture of 20 μ M of SP and compound Z-3578 (1, 5, and 10 μ M) was added to LAD2 cells (1×10^6 /well) using medium as a solvent, and the cells were incubated for 6 h. For blank group, cells were treated with medium instead of any compound. The supernatant was collected for the ELISA kit assay.

Paw Swelling and Evans Blue Extravasation Assay. The C57 mice were randomly divided into the treated group (0.1, 0.5, and 1 mg/mL) and the C48/80 group, five mice in each group. A solution (0.2 mL) at a concentration of 0.1, 0.5, and 1 mg/mL of compounds and the same volume of solvent were administered by gavage to the treated and C48/80 groups. Two hours later, the mice were anesthetized by 25 mg/kg sodium pentobarbital intraperitoneally and injected with 0.2 mL of 0.4% Evans blue in saline by tail intravenous. The thickness of the left and right paws (La and Ra) was measured for the first time by the Vernier caliper. Then, 5 μ L of saline and 60 μ g/mL C48/80 were injected into the left and right soles of mice, respectively. The paw thickness was recorded again after 15 min, and then, the mice were anesthetized and sacrificed by cervical dislocation, decapitated, and executed. Photographs of the paws were taken, and the right and left paws were clipped off in 1.5 mL EP tubes and dried overnight at 60 $^{\circ}$ C. Each paw was weighed, and 450 μ L of acetone/saline (7:3) was added to the tube. The paw tissue was cut, sonicated, and centrifuged to obtain the supernatant. The OD value of each well was measured at 620 nm.

Serum Histamine Assay in Mice. The C57 mice were randomly divided into the treated group (1, 5, and 10 mg/mg), the C48/80 group, and control group (five mice in each group). The experimental gavage method was consistent with the detection of paw swelling and Evans blue extravasation in mice. Two hours later, mice were injected with 0.2 mL of 30 μ g/mL C48/80 in saline by tail intravenous. After 1 h, 0.5 mL of blood was collected from the eyes of the mice and placed in EP tubes containing 1% sodium heparin. The blood was centrifuged at 12,000 rpm for 20 min at 4 $^{\circ}$ C to obtain the serum. The *d*₄-HA (serum: *d*₄-HA = 1:2 (V/V)) was added, mixed, centrifuged, and filtered for mass spectrometry detection by UHPLC-ESI-MS/MS.

Skin Toluidine Blue Staining in Mice. The C57 mice were randomly divided into the treated (10 mg/kg), the C48/80, and the control groups. A solution (0.2 mL) at the concentration of 1 mg/mL of compound was administered by gavage to the treated. The same volume of solvent was administered to C48/80 and the control groups. Two hours later, the mice were anesthetized by 25 mg/kg sodium pentobarbital intraperitoneally. Also, 5 μ L of saline and 100 μ g/mL C48/80 were injected into the left and right soles of mice. After 15 min, the mice were sacrificed, and the skin tissue of the paw was cut off and fixed by immersion in 4% paraformaldehyde. Next, the skin tissue was embedded, sectioned, deparaffinized, antigen-repaired, and blocked. Then the skin tissue was stained with toluidine blue and sealed, and images were immediately taken using an ECLIPSE Ci-L orthotopic imaging microscope (Nikon, Tokyo, Japan).

Frontal Analysis. The equilibrium dissociation constant (K_D) reflects the affinity between the ligand and receptor, and the K_D value is determined using the frontal method analysis.⁴⁸ Initially, 20 mM Na₂HPO₄ buffer solution served as a mobile phase A, and the compound Z-3578 was dissolved in mobile phase A as mobile phase B. By adjusting the ratio of mobile phase A and B, the concentrations of compound Z-3578 ranging from 2×10^{-7} to 1×10^{-6} mol/L were achieved. After equilibration of the MrgX2-His-tag@VS column, compound Z-3578 was sequentially introduced into the equilibrated column from low to high concentrations. Once the breakthrough

curve was reached, the column was returned to equilibrium with mobile phase A before proceeding with the next concentration. The K_D value was calculated through the previous literature.⁴⁸

Zonal Elution. The zonal elution study of cell membrane chromatography was used as described.⁴⁹ Briefly, 5 mM Na_2HPO_4 buffer solution as mobile phase A and (R)-ZINC-3573 in maximal concentration were added in 5 mM Na_2HPO_4 buffer solution as mobile phase B. By adjusting the ratio of mobile phase A and B, the concentrations of (R)-ZINC-3573 ranging from 0 to 1×10^{-7} mol/L were achieved. Also, the retentions of Z-3578 to be measured were recorded.

Surface Plasmon Resonance. Surface plasmon resonance (SPR) tests were performed to evaluate the interaction strength between Z-3578 and MrgX2. Target proteins were immobilized on the CM5 sensor chip (Cytiva, USA) and 5% SDS running buffer (SDS dissolved in $1.05 \times \text{PBS-P}$) at a flow rate of 30 $\mu\text{L}/\text{min}$. Serial dilutions of Z-3578 with concentrations ranging from 0.195 to 3.125 μM were run through, and the chip was regenerated with glycine 2.0. The resulting data were fitted to a 1:1 binding model and analyzed by Biacore T200 software.

Molecular Docking. The compound structure was drawn by the program ChemDraw 21.0.0 and transformed into the MOL2 format by Chem3D 8.0. Then, the compound was depicted and optimized by Powell's method with a Tripos force field with a convergence criterion at 0.05 kcal/(Å mol) and assigned with Gasteiger–Hückel method by SYBYL-X 2.0. The MrgX2 model was downloaded from PDB BANK (PDB code: 7S8O). Dehydrate and hydrogenation of the protein were done using SYBYL-X 2.0 to create an active pocket. Semiflexible molecular docking of the optimized small molecules was performed with the protein. The results were visualized using PyMOL (<https://pymol.org/2/>).

Statistical Analysis. All results are presented by mean \pm SEM, and significant differences were calculated by one-way ANOVA and unpaired *t* tests. Differences were considered significant at **P* < 0.05, ***P* < 0.01, and ****P* < 0.001.

■ ASSOCIATED CONTENT

Data Availability Statement

Data will be made available on request.

Supporting Information

The Supporting Information is available free of charge at <https://pubs.acs.org/doi/10.1021/acs.jmedchem.5c00258>.

Molecular Formula Strings Spreadsheet (CSV)

■ AUTHOR INFORMATION

Corresponding Author

Cheng Wang – School of Pharmacy, Health Science Center, Xi'an Jiaotong University, Xi'an, Shaanxi 710061, China; orcid.org/0000-0002-0178-8317; Email: chengwang@xjtu.edu.cn

Authors

Zhaomin Xia – School of Pharmacy, Health Science Center, Xi'an Jiaotong University, Xi'an, Shaanxi 710061, China

Qiumei Zhu – The 920th Hospital of Chinese People's Liberation Army Joint Logistics Support Force, Kunming, Yunnan 650100, China

Yi Shan – School of Pharmacy, Health Science Center, Xi'an Jiaotong University, Xi'an, Shaanxi 710061, China

Jiayu Lu – School of Pharmacy, Health Science Center, Xi'an Jiaotong University, Xi'an, Shaanxi 710061, China

Meidi An – School of Pharmacy, Health Science Center, Xi'an Jiaotong University, Xi'an, Shaanxi 710061, China

Xiaoxue Mo – School of Pharmacy, Health Science Center, Xi'an Jiaotong University, Xi'an, Shaanxi 710061, China

Siqi Wang – School of Pharmacy, Health Science Center, Xi'an Jiaotong University, Xi'an, Shaanxi 710061, China

Wen Yang – School of Pharmacy, Health Science Center, Xi'an Jiaotong University, Xi'an, Shaanxi 710061, China

Hua Qian – Department of Cardiology, The First Affiliated Hospital of Xi'an Jiaotong University, Xi'an, Shaanxi 710061, China

Huaizhen He – School of Pharmacy, Health Science Center, Xi'an Jiaotong University, Xi'an, Shaanxi 710061, China;

orcid.org/0000-0002-2836-2308

Complete contact information is available at:

<https://pubs.acs.org/10.1021/acs.jmedchem.5c00258>

Author Contributions

#Z.X. and Q.Z. contributed equally to this work

Author Contributions

Z.X. was responsible for data curation, investigation, formal analysis, validation, visualization, writing—original draft, and software. Q.Z. was responsible for investigation, validation, writing—original draft, and software. Y.S. and J.L. were responsible for investigation, validation, and software. M.A., X.M., S.W., and W.Y. were responsible for validation. H.Q. was responsible for methodology. H.H. was responsible for supervision and funding acquisition. C.W. was responsible for writing—review and editing, and project administration.

Notes

The authors declare no competing financial interest.

■ ACKNOWLEDGMENTS

This research was supported by National Natural Science Foundation of China (nos. 82373830; 81930096); the Natural Science Basic Research Plan in Shanxi Province of China (no. 2023-JC-YB-679); the Special Practical Teaching Project of Xi'an Jiaotong University for Medical Undergraduates 2023 (project no. 23SJZX-B12).

■ REFERENCES

- (1) Al Hamwi, G.; Riedel, Y. K.; Clemens, S.; Namasivayam, V.; Thimm, D.; Muller, C. E. MAS-related G protein-coupled receptors X (MRGPRX): Orphan GPCRs with potential as targets for future drugs. *Pharmacol. Ther.* **2022**, 238, No. 108259.
- (2) Subramanian, H.; Gupta, K.; Ali, H. Roles of Mas-related G protein-coupled receptor X2 on mast cell-mediated host defense, pseudoallergic drug reactions, and chronic inflammatory diseases. *J. Allergy Clin. Immunol.* **2016**, 138 (3), 700–710.
- (3) Tatamoto, K.; Nozaki, Y.; Tsuda, R.; Konno, S.; Tomura, K.; Furuno, M.; Ogasawara, H.; Edamura, K.; Takagi, H.; Iwamura, H.; et al. Immunoglobulin E-independent activation of mast cell is mediated by Mrg receptors. *Biochem. Biophys. Res. Commun.* **2006**, 349 (4), 1322–1328.
- (4) Serhan, N.; Basso, L.; Sibilano, R.; Petitfils, C.; Meixiong, J.; Bonnard, C.; Reber, L. L.; Marichal, T.; Starkl, P.; Cenac, N.; et al. House dust mites activate nociceptor–mast cell clusters to drive type 2 skin inflammation. *Nat. Immunol.* **2019**, 20 (11), 1435–1443.
- (5) Fujisawa, D.; Kashiwakura, J. i.; Kita, H.; Kikukawa, Y.; Fujitani, Y.; Sasaki-Sakamoto, T.; Kuroda, K.; Nunomura, S.; Hayama, K.; Terui, T.; Ra, C.; Okayama, Y.; et al. Expression of Mas-related gene X2 on mast cells is upregulated in the skin of patients with severe chronic urticaria. *J. Allergy Clin. Immunol.* **2014**, 134 (3), 622–633.
- (6) McNeil, B. D.; Pundir, P.; Meeker, S.; Han, L.; Udem, B. J.; Kulka, M.; Dong, X. Identification of a mast-cell-specific receptor crucial for pseudo-allergic drug reactions. *Nature.* **2015**, 519 (7542), 237–241.

- (7) Wang, N.; Che, D.; Zhang, T.; Liu, R.; Cao, J.; Wang, J.; Zhao, T.; Ma, P.; Dong, X.; He, L. Saikosaponin A inhibits compound 48/80-induced pseudo-allergy via the Mrgprx2 pathway in vitro and in vivo. *Biochem. Pharmacol.* **2018**, *148*, 147–154.
- (8) Wang, N.; Wang, J.; Zhang, Y.; Zeng, Y.; Hu, S.; Bai, H.; Hou, Y.; Wang, C.; He, H.; He, L. Imperatorin ameliorates mast cell-mediated allergic airway inflammation by inhibiting MRGPRX2 and CamKII/ERK signaling pathway. *Biochem. Pharmacol.* **2021**, *184*, No. 114401.
- (9) Ding, Y.; Ma, T.; Zhang, Y.; Zhao, C.; Wang, C.; Wang, Z. Rosmarinic acid ameliorates skin inflammation and pruritus in allergic contact dermatitis by inhibiting mast cell-mediated MRGPRX2/PLC γ 1 signaling pathway. *Int. Immunopharmacol.* **2023**, *117*, No. 110003.
- (10) Wollam, J.; Solomon, M.; Villescaz, C.; Lanier, M.; Evans, S.; Bacon, C.; Freeman, D.; Vasquez, A.; Vest, A.; Npora, J.; et al. Inhibition of mast cell degranulation by novel small molecule MRGPRX2 antagonists. *J. Allergy Clin. Immunol.* **2024**, *154* (4), 1033–1043.
- (11) Wang, C.; Hu, T.; Lu, J.; Lv, Y.; Ge, S.; Hou, Y.; He, H. Convenient diaryl ureas as promising anti-pseudo-allergic agents. *J. Med. Chem.* **2022**, *65* (15), 10626–10637.
- (12) Lu, J.; Xia, Z.; Zhang, Y.; Wang, H.; Yang, W.; Wang, S.; Wang, N.; Liu, Y.; He, H.; Wang, C.; et al. Relative symmetry with electronegativity of different key-groups” strategy for MRGPRX2 antagonist design and its effect on antigen-induced pulmonary inflammation. *Acta. Pharm. Sin. B* **2025**, *15* (1), 494–507.
- (13) Wang, C.; Hou, Y.; Ge, S.; Lu, J.; Wang, X.; Lv, Y.; Wang, N.; He, H. Synthetic imperatorin derivatives alleviate allergic reactions via mast cells. *Biomed. Pharmacother.* **2022**, *150*, No. 112982.
- (14) Kumar, M.; Duraisamy, K.; Annapureddy, R. R.; Chan, C. B.; Chow, B. K. C. Novel small molecule MRGPRX2 antagonists inhibit a murine model of allergic reaction. *J. Allergy Clin. Immunol.* **2023**, *151* (4), 1110–1122.
- (15) Wong, T. K.; Choi, Y. G.; Li, P. H.; Chow, B. K. C.; Kumar, M. MRGPRX2 antagonist GE1111 attenuated DNFB-induced atopic dermatitis in mice by reducing inflammatory cytokines and restoring skin integrity. *Front. Immunol.* **2024**, *15*, 1406438.
- (16) Suzuki, Y.; Liu, S.; Ogasawara, T.; Sawasaki, T.; Takasaki, Y.; Yorozuya, T.; Mogi, M. A novel MRGPRX2-targeting antagonistic DNA aptamer inhibits histamine release and prevents mast cell-mediated anaphylaxis. *Eur. J. Pharmacol.* **2020**, *878*, No. 173104.
- (17) Dondalska, A.; Rönnerberg, E.; Ma, H.; Pålsson, S. A.; Magnusdottir, E.; Gao, T.; Adam, L.; Lerner, E. A.; Nilsson, G.; Lagerström, M.; et al. Amelioration of compound 48/80-mediated itch and LL-37-Induced inflammation by a single-stranded oligonucleotide. *Front. Immunol.* **2020**, *11*, No. 559589.
- (18) Pinzi, L.; Rastelli, G. Molecular Docking: Shifting Paradigms in Drug Discovery. *Int. J. Mol. Sci.* **2019**, *20* (18), 4331.
- (19) Du, J.; Guo, J.; Kang, D.; Li, Z.; Wang, G.; Wu, J.; Zhang, Z.; Fang, H.; Hou, X.; Huang, Z.; et al. New techniques and strategies in drug discovery. *Chin. Chem. Lett.* **2020**, *31* (7), 1695–1708.
- (20) Serrano, D. R.; Luciano, F. C.; Anaya, B. J.; Ongoren, B.; Kara, A.; Molina, G.; Ramirez, B. I.; Sánchez-Guirales, S. A.; Simon, J. A.; Tomietto, G.; et al. Artificial intelligence (AI) applications in drug discovery and drug delivery: revolutionizing personalized medicine. *Pharmaceutics* **2024**, *16* (10), 1328.
- (21) Katona, É.; Péntes, K.; Csapó, A.; Fazakas, F.; Udvardy, M. L.; Bagoly, Z.; Orosz, Z. Z.; Muszbek, L. Interaction of factor XIII subunits. *Blood* **2014**, *123* (11), 1757–1763.
- (22) Falconer, R. J.; Penkova, A.; Jelesarov, I.; Collins, B. M. Survey of the year 2008: applications of isothermal titration calorimetry. *J. Mol. Recognit.* **2010**, *23* (5), 395–413.
- (23) Stanisavljevic, M.; Krizkova, S.; Vaculovicova, M.; Kizek, R.; Adam, V. Quantum dots-fluorescence resonance energy transfer-based nanosensors and their application. *Biosensors and Bioelectron.* **2015**, *74*, 562–574.
- (24) Ma, W.; Wang, C.; Liu, R.; Wang, N.; Lv, Y.; Dai, B.; He, L. Advances in cell membrane chromatography. *J. Chromatogr. A* **2021**, *1639*, No. 461916.
- (25) He, L.; Wang, S.; Geng, X. Coating and fusing cell membranes onto a silica surface and their chromatographic characteristics. *Chromatographia* **2001**, *54* (1), 71–76.
- (26) Bu, Y.; Hu, Q.; Bao, T.; Xie, X.; Wang, S. Recent advances in cell membrane-coated technology for drug discovery from natural products. *TrAC. Trends in Anal. Chem.* **2022**, *151*, No. 116601.
- (27) Steen Redeker, E.; Ta, D. T.; Cortens, D.; Billen, B.; Guedens, W.; Adriaenssens, P. Protein engineering for directed immobilization. *Bioconjug Chem.* **2013**, *24* (11), 1761–1777.
- (28) Lai, Y.-T.; Chang, Y.-Y.; Hu, L.; Yang, Y.; Chao, A.; Du, Z.-Y.; Tanner, J. A.; Chye, M.-L.; Qian, C.; Ng, K.-M.; et al. Rapid labeling of intracellular His-tagged proteins in living cells. *Proc. Natl. Acad. Sci. U S A* **2015**, *112* (10), 2948–2953.
- (29) Gao, X.; Li, Y.; Qin, Y.; Chen, E.; Li, Q.; Zhao, X.; Bian, L.; Zheng, J.; Li, Z.; Zhang, Y.; et al. Reversible and oriented immobilization of histidine-tagged protein on silica gel characterized by frontal analysis. *RSC. Adv.* **2015**, *5* (31), 24449–24454.
- (30) Dörr, J. M.; Scheidelaar, S.; Koorengel, M. C.; Dominguez, J. J.; Schäfer, M.; van Walree, C. A.; Killian, J. A. The styrene–maleic acid copolymer: a versatile tool in membrane research. *Eur. Biophys. J.* **2016**, *45* (1), 3–21.
- (31) Postis, V.; Rawson, S.; Mitchell, J. K.; Lee, S. C.; Parslow, R. A.; Dafforn, T. R.; Baldwin, S. A.; Muench, S. P. The use of SMALPs as a novel membrane protein scaffold for structure study by negative stain electron microscopy. *Biochim. Biophys. Acta* **2015**, *1848* (2), 496–501.
- (32) Pollock, N. L.; Rai, M.; Simon, K. S.; Hesketh, S. J.; Teo, A. C. K.; Parmar, M.; Sridhar, P.; Collins, R.; Lee, S. C.; Stroud, Z. N.; et al. SMA-PAGE: A new method to examine complexes of membrane proteins using SMALP nano-encapsulation and native gel electrophoresis. *Biochim. Biophys. Acta. Biomembr.* **2019**, *1861* (8), 1437–1445.
- (33) Kopf, A. H.; Koorengel, M. C.; van Walree, C. A.; Dafforn, T. R.; Killian, J. A. A simple and convenient method for the hydrolysis of styrene-maleic anhydride copolymers to styrene-maleic acid copolymers. *Chem. Phys. Lipids* **2019**, *218*, 85–90.
- (34) Logez, C.; Damian, M.; Legros, C.; Dupré, C.; Guéry, M.; Mary, S.; Wagner, R.; M’Kadmi, C.; Nosjean, O.; Fould, B.; et al. Detergent-free isolation of functional G protein-coupled receptors into nanometric lipid particles. *Biochemistry* **2016**, *55* (1), 38–48.
- (35) Morrison, K. A.; Akram, A.; Mathews, A.; Khan, Z. A.; Patel, J. H.; Zhou, C.; Hardy, D. J.; Moore-Kelly, C.; Patel, R.; Odiba, V.; et al. Membrane protein extraction and purification using styrene–maleic acid (SMA) copolymer: effect of variations in polymer structure. *Biochem. J.* **2016**, *473* (23), 4349–4360.
- (36) Li, M.; Cheng, F.; Li, H.; Jin, W.; Chen, C.; He, W.; Cheng, G.; Wang, Q. Site-specific and covalent immobilization of His-Tagged proteins via surface vinyl sulfone–imidazole coupling. *Langmuir.* **2019**, *35* (50), 16466–16475.
- (37) Ge, S.; Wang, C.; Si, M.; Zhu, Q.; Shan, Y.; Li, N.; Wang, Y.; Wang, H.; Luo, G.; He, H.; et al. Site-specific covalent immobilization of SMA-stabilized ACE2 for SARS-CoV-2 recognition and drug screening. *ACS. Appl. Mater. Interfaces* **2023**, *15* (28), 33348–33361.
- (38) Krystal-Whittemore, M.; Dileepan, K. N.; Wood, J. G. Mast Cell: A multi-functional master cell. *Front. Immunol.* **2016**, *6*, 620.
- (39) Theoharides, T. C.; Alysandratos, K.-D.; Angelidou, A.; Delivanis, D.-A.; Sismanopoulos, N.; Zhang, B.; Asadi, S.; Vasiadi, M.; Weng, Z.; Miniati, A.; et al. Mast cells and inflammation. *Biochim. Biophys. Acta* **2012**, *1822* (1), 21–33.
- (40) Green, D. P.; Limjunyawong, N.; Gour, N.; Pundir, P.; Dong, X. A mast-cell-specific receptor mediates neurogenic inflammation and pain. *Neuron* **2019**, *101* (3), 412–420.
- (41) Berridge, M. J.; Bootman, M. D.; Roderick, H. L. Calcium signalling: dynamics, homeostasis and remodelling. *Nat. Rev. Mol. Cell. Biol.* **2003**, *4* (7), 517–529.

(42) Calleri, E.; Temporini, C.; Massolini, G. Frontal affinity chromatography in characterizing immobilized receptors. *J. Pharm. Biomed. Anal.* **2011**, *54* (5), 911–925.

(43) Sanghvi, M.; Moaddel, R.; Wainer, I. W. The development and characterization of protein-based stationary phases for studying drug–protein and protein–protein interactions. *J. Chromatogr. A* **2011**, *1218* (49), 8791–8798.

(44) Yang, F.; Guo, L.; Li, Y.; Wang, G.; Wang, J.; Zhang, C.; Fang, G. X.; Chen, X.; Liu, L.; Yan, X.; Liu, Q.; Qu, C.; Xu, Y.; Xiao, P.; Zhu, Z.; Li, Z.; Zhou, J.; Yu, X.; Gao, N.; Sun, J. P.; et al. Structure, function and pharmacology of human itch receptor complexes. *Nature* **2021**, *600* (7887), 164–169.

(45) Cao, C.; Kang, H. J.; Singh, I.; Chen, H.; Zhang, C.; Ye, W.; Hayes, B. W.; Liu, J.; Gumpfer, R. H.; Bender, B. J.; et al. Structure, function and pharmacology of human itch GPCRs. *Nature* **2021**, *600* (7887), 170–175.

(46) Elst, J.; Maurer, M.; Sabato, V.; Faber, M. A.; Bridts, C. H.; Mertens, C.; Van Houdt, M.; Van Gasse, A. L.; van der Poorten, M.-L. M.; De Puyseleir, L. P.; et al. Novel insights on MRGPRX2-mediated hypersensitivity to neuromuscular blocking agents and fluoroquinolones. *Front. Immunol.* **2021**, *12*, No. 668962.

(47) Liu, R.; Che, D.; Zhao, T.; Pundir, P.; Cao, J.; Lv, Y.; Wang, J.; Ma, P.; Fu, J.; Wang, N.; et al. MRGPRX2 is essential for sinomenine hydrochloride induced anaphylactoid reactions. *Biochem. Pharmacol.* **2017**, *146*, 214–223.

(48) Ma, W.; Yang, L.; He, L. Overview of the detection methods for equilibrium dissociation constant K_D of drug-receptor interaction. *J. Pharm. Anal.* **2018**, *8* (3), 147–152.

(49) Ma, W.; Yang, L.; Lv, Y.; Fu, J.; Zhang, Y.; He, L. Determine equilibrium dissociation constant of drug-membrane receptor affinity using the cell membrane chromatography relative standard method. *J. Chromatogr. A* **2017**, *1503*, 12–20.



CAS BIOFINDER DISCOVERY PLATFORM™

ELIMINATE DATA SILOS. FIND WHAT YOU NEED, WHEN YOU NEED IT.

A single platform for relevant, high-quality biological and toxicology research

Streamline your R&D

CAS
A Division of the American Chemical Society